C. R. Mecanique 343 (2015) 331–343

Contents lists available at ScienceDirect

Comptes Rendus Mecanique

www.sciencedirect.com

The incremental Cauchy Problem in elastoplasticity: General solution method and semi-analytic formulae for the pressurised hollow sphere ☆

Thouraya Nouri Baranger [a,*], Stéphane Andrieux [b,*], Thi Bach Tuyet Dang [a]

[a] Université de Lyon, CNRS, LMC2 Université Lyon-1, LaMCoS UMR5259, 15, boulevard Laterjet, 69622, Villeurbanne cedex, France
[b] LaMSID, UMR EDF–CNRS–CEA 8193, 1, avenue du Général-de-Gaulle, 92141, Clamart cedex, France

ARTICLE INFO

Article history:
Received 12 January 2015
Accepted 14 April 2015
Available online 5 May 2015

Keywords:
Inverse problem
Cauchy Problem
Plasticity
Data completion
Constitutive Law Error
Linear-hardening

ABSTRACT

A general solution method to the Cauchy Problem (CP) formulated for incremental elastoplasticity is designed. The method extends previous works of the authors on the solution to Cauchy Problems for linear operators and convex nonlinear elasticity in small strain to the case of generalised standard materials defined by two convex potentials. The CP is transformed into the minimisation of an error between the solutions to two well-posed elastoplastic evolution problems. A one-parameter family of errors in the constitutive equation is derived based on Legendre–Fenchel residuals. The method is illustrated by the simple example of a pressurised thick-spherical reservoir made of elastic, linear strain-hardening plastic material. The identification of inner pressure and plasticity evolution has been carried-out using semi-analytical solutions to the elastoplastic behaviours to build the error functional.

1. Introduction

The issue of recovering missing data on inaccessible parts of the boundary of a solid, provided some information is given on the remaining part, which can be formulated as a Cauchy Problem or as a data completion problem, has been widely investigated in the framework of elliptic problem with linear isotropic media. Various methods have been proposed in the literature in order to solve this issue; without being exhaustive, one can cite the front propagation method by Bui [1,2], Bonnet and Bui [3], the moment method by Hon and Wei [4], the fixed point algorithm by Kozlov et al. [5], the evanescent regularisation by Cimetière et al. [6], the quasi-reversibility approach developed first by Lattes and Lions [7] and recently by Bourgeois [8], the boundary elements and the fundamental solution methods by Marin and Lesnic [9,10]; finally, Ghnatios et al. [11] used the Proper Generalised Decomposition method in the case of a one-dimensional heat transfer problem. A large amount of work addresses only homogeneous and linear isotropic media. In the nonlinear framework, Stolz [12] applied optimal control approach to solve the Cauchy Problem in the framework of elasto-viscoplasticity with a least square error functional. Kugler and Leitão [13] and Egger and Leitão [14] studied the existence of a solution to the nonlinear Cauchy Problem by constructive method using a fixed point algorithm.

☆ Cauchy Problem for Elastoplasticity.

* Corresponding authors.
E-mail addresses: Thouraya.baranger@univ-lyon1.fr (T.N. Baranger), Stephane.Andrieux@edf.fr (S. Andrieux).

http://dx.doi.org/10.1016/j.crme.2015.04.002
1631-0721/

In Baranger and Andrieux [15], the authors suggested to formulate the issue as a constrained optimisation problem. Addressing the problem for the Laplace operator as a model of scalar conduction phenomena, the method relies on the definition and solution to two usual well-posed problems and the minimisation of the gap between the two solutions defined as a pseudo-energy error functional. It was showed furthermore that the iterated resolutions algorithm of Kozlov et al. [5] (the KMF algorithm), used by various authors such Leitão [16] and Marin [17], can be interpreted for linear symmetric operators as an alternating directions descent method for the minimisation error functional introduced. This result explains a remarkable performance of the proposed method with respect to the KMF algorithm and allows dealing with full 3D situations for heterogeneous and anisotropic solids.

The method has been developed for other linear operators, as the Lamé operator for linear infinitesimal elasticity with various applications such as determination of contact zones, identification of inclusions or determination of the stress state on buried interfaces in Baranger and Andrieux [18] and in [19–22]. Linear parabolic or hyperbolic operators have also been addressed with an appropriate extension for the definition of the energy error functional [23–25]. As the Cauchy Problem is well known to be severely ill posed (Hadamard [26], Belgacem [27]), regularisation procedures have also been studied and some regularisation has been added to the solution to the Cauchy Problem by energy error minimisation without modifying the functional itself.

Recently, a new extension of the approach to non-linear problems has been proposed for the case of hyperelasticity. The error functional is no more an energy error between the two solutions to well-posed problems, but rather an error in the constitutive equation that takes advantage of the existence of a convex, lower semi-continuous (*lsc*) energy potential entering into the formulation of the hyperelastic constitutive relation (Andrieux and Baranger [28] and in [29]).

This paper is devoted to an extension of the method in a different direction, namely the (incremental) plasticity, involving dissipative and memory effects. The next part recalls the framework used for the description of hardening and perfect plasticity and the formulation of the data completion problem in this context. Then the definition of the two intermediate boundary value problems is given and the derivation of various possibilities for the error in constitutive equation is detailed. An illustration of the method is performed in the last section in the case of the simple situation of a pressurised spherical reservoir.

2. The Cauchy Problem for incremental plasticity

Adopting the framework of generalised standard materials Halphen and Nguyen [30], the general constitutive equations for elastoplasticity is obtained, involving the three following ingredients:

- a set of state variables $(\boldsymbol{\epsilon}, \boldsymbol{\epsilon}^{\mathrm{p}}, \boldsymbol{\alpha})$ where $\boldsymbol{\epsilon}$ is the linearised strain tensor, $\boldsymbol{\epsilon}^{\mathrm{p}}$ the (additive) plastic strain and α a set of additional internal variables, possibly empty for perfect plasticity;
- a convex, lsc, differentiable free (or stored internal) energy density: $W(\boldsymbol{\epsilon} - \boldsymbol{\epsilon}^{\mathrm{p}}, \boldsymbol{\alpha})$
- a convex, lsc, positively 1-homogeneous potential of dissipation: $\Psi(\dot{\boldsymbol{\epsilon}}^{\mathrm{p}}, \dot{\boldsymbol{\alpha}}; \boldsymbol{\epsilon}^{\mathrm{p}}, \boldsymbol{\alpha})$

and reads:

$$\boldsymbol{\sigma} = \frac{\partial W}{\partial \boldsymbol{\epsilon}} = -\frac{\partial W}{\partial \boldsymbol{\epsilon}^{\mathrm{p}}}, \quad \mathbf{A} = -\frac{\partial W}{\partial \boldsymbol{\alpha}} \tag{1}$$

$$\boldsymbol{\sigma} \in \partial_{\dot{\boldsymbol{\epsilon}}^{\mathrm{p}}} \Psi \ , \ \mathbf{A} \in \partial_{\dot{\boldsymbol{\alpha}}} \Psi \tag{2}$$

where $\boldsymbol{\sigma}$ is the stress tensor, and $\partial_{\mathbf{x}} \Psi$ stands for the sub-differential of Ψ with respect to $\mathbf{x}$. As Ψ is positively 1-homogeneous, (2) is equivalent to the normality rule for $(\dot{\boldsymbol{\epsilon}}^{\mathrm{p}}, \dot{\boldsymbol{\alpha}})$ with respect to a convex yield function $f(\dot{\boldsymbol{\sigma}}^{\mathrm{p}}, \dot{\boldsymbol{A}}) \leq 0$. This framework encompasses a large amount of associated plasticity laws and ensures that the Clausius–Duhem inequality is fulfilled. In applications, the time interval is discretized into finite time increments, then the incremental form of the preceding equation is chosen as the total implicit one. This choice maintains the existence of a global incremental convex variation form of the evolution equation (for positive hardening behaviour), see Mialon [31], Simo and Hughes [32]. The implicit incremental form is then:

$$\begin{cases} \boldsymbol{\sigma} + \Delta\boldsymbol{\sigma} = \dfrac{\partial W}{\partial \boldsymbol{\epsilon}}(\boldsymbol{\epsilon} + \Delta\boldsymbol{\epsilon} - \boldsymbol{\epsilon}^{\mathrm{p}} - \Delta\boldsymbol{\epsilon}^{\mathrm{p}}, \boldsymbol{\alpha} + \Delta\boldsymbol{\alpha}), \quad \boldsymbol{\sigma} + \Delta\boldsymbol{\sigma} \in \partial_{\dot{\boldsymbol{\epsilon}}^{\mathrm{p}}} \Psi(\Delta\boldsymbol{\epsilon}^{\mathrm{p}}, \Delta\boldsymbol{\alpha}; \boldsymbol{\epsilon}^{\mathrm{p}} + \Delta\boldsymbol{\epsilon}^{\mathrm{p}}, \boldsymbol{\alpha} + \Delta\boldsymbol{\alpha}) \quad \text{(a)} \\ \mathbf{A} + \Delta\mathbf{A} = -\dfrac{\partial W}{\partial \boldsymbol{\alpha}}(\boldsymbol{\epsilon} + \Delta\boldsymbol{\epsilon} - \boldsymbol{\epsilon}^{\mathrm{p}} - \Delta\boldsymbol{\epsilon}^{\mathrm{p}}, \boldsymbol{\alpha} + \Delta\boldsymbol{\alpha}), \quad \mathbf{A} + \Delta\mathbf{A} \in \partial_{\dot{\boldsymbol{\alpha}}} \Psi(\Delta\boldsymbol{\epsilon}^{\mathrm{p}}, \Delta\alpha; \boldsymbol{\epsilon}^{\mathrm{p}} + \Delta\boldsymbol{\epsilon}^{\mathrm{p}}, \boldsymbol{\alpha} + \Delta\boldsymbol{\alpha}) \quad \text{(b)} \end{cases} \tag{3}$$

For the sake of simplicity, we shall drop the arguments of the potentials. Consider now the following data completion problem. Given a solid Ω, its boundary consists of two non-overlapping parts Γ_{m} and Γ_{u} with unit external normal $\mathbf{n}$. On Γ_{u} no data are available, whereas on Γ_{m} both the displacement field $\mathbf{u} = \mathbf{U}_{\mathrm{m}}$ and the stress vector field $\boldsymbol{\sigma}.\mathbf{n} = \mathbf{F}_{\mathrm{m}}$ are given.

The typical situation is the case where the displacement field $\mathbf{U}_{\mathrm{m}}$ (eventually only its tangential part) is obtained from digital image correlation techniques on a surface free of charge ($\mathbf{F}_{\mathrm{m}} = 0$). Frequently, in real applications, there is a third part of the boundary where natural or essential boundary conditions are known, but, for the sake of simplicity, we shall derive the formulation of the problem with only the two complementary parts Γ_{m} and Γ_{u}. The data completion problem

is to recover the data on Γ_u provided the equilibrium equation, the compatibility condition and the evolution equation (3) inside the solids hold true:

$$\nabla \cdot [\boldsymbol{\sigma} + \Delta\boldsymbol{\sigma}] = 0, \quad \boldsymbol{\epsilon}(\mathbf{u} + \Delta\mathbf{u}) = [\nabla(\mathbf{u} + \Delta\mathbf{u})]^{\text{sym}} \tag{4}$$

Strictly speaking, the Cauchy Problem is the determination of a displacement field $\Delta\mathbf{u}$ inside the solid Ω, fulfilling (3) and (4) and satisfying the two boundary conditions on Γ_m: $\Delta\mathbf{u} = \Delta\mathbf{U}_m$ and $\Delta\boldsymbol{\sigma}(\mathbf{u}).\mathbf{n} = \Delta\mathbf{F}_m$. In the sequel, the solution method will take as unknown the displacement or the normal stress vector on Γ_u. So it can be considered that a (partial) data completion is tackled with. But as far as the solution method relies on the production of vector fields $(\mathbf{u}, \boldsymbol{\sigma})$ fulfilling the evolution equation for the solid, we can speak either of data completion solution or of solution to the Cauchy Problem.

3. Derivation of the error minimisation method

To solve the above Cauchy or data completion problem over a time interval Δt, two auxiliary usual elastoplastic evolution sub-problems $\mathcal{P}_i$ are defined, using only one of the overspecified boundary data $\Delta\mathbf{U}_m$ or $\Delta\mathbf{F}_m$ on Γ_m and a given normal stress vector field $\Delta\eta$ on Γ_u, the solutions to which are denoted by $(\Delta\mathbf{u}_1, \Delta\boldsymbol{\sigma}_1)$ and $(\Delta\mathbf{u}_2, \Delta\boldsymbol{\sigma}_2)$. The common initial state at the beginning of the time increment is $(\mathbf{u}, \boldsymbol{\sigma}, \boldsymbol{\epsilon}^p, \boldsymbol{\alpha})$.

$$\begin{cases} \nabla \cdot [\boldsymbol{\sigma} + \Delta\boldsymbol{\sigma}_i] = 0, \quad \boldsymbol{\epsilon}(\mathbf{u} + \Delta\mathbf{u}_i) = [\nabla(\mathbf{u} + \Delta\mathbf{u}_i)]^{\text{sym}} \\ \boldsymbol{\sigma} + \Delta\boldsymbol{\sigma}_i = \frac{\partial W}{\partial \boldsymbol{\epsilon}}, \quad \mathbf{A} + \Delta\mathbf{A}_i = -\frac{\partial W}{\partial \boldsymbol{\alpha}} \qquad \text{for} \quad i = 1, 2 \\ \boldsymbol{\sigma} + \Delta\boldsymbol{\sigma}_i \in \partial_{\dot{\boldsymbol{\epsilon}}^p} \Psi(\Delta\boldsymbol{\epsilon}_i^p, \Delta\boldsymbol{\alpha}_i) \end{cases} \tag{5}$$

and respectively for $\mathcal{P}_1$ and $\mathcal{P}_2$:

$$(\mathcal{P}_1) \begin{cases} \Delta\mathbf{u}_1 = \Delta\mathbf{U}_m \text{ on } \Gamma_m \\ \Delta\boldsymbol{\sigma}_1 \cdot \mathbf{n} = \Delta\boldsymbol{\eta} \text{ on } \Gamma_u \end{cases} \quad \text{and} \quad (\mathcal{P}_2) \begin{cases} \Delta\boldsymbol{\sigma}_2 \cdot \mathbf{n} = \Delta\mathbf{F}_m \text{ on } \Gamma_m \\ \Delta\boldsymbol{\sigma}_2 \cdot \mathbf{n} = \Delta\boldsymbol{\eta} \text{ on } \Gamma_u \end{cases} \tag{6}$$

It is now clear that if the increment of surface traction $\Delta\boldsymbol{\eta}$ is such that $\Delta\mathbf{u}_1 = \Delta\mathbf{u}_2 + RBM$, where RBM is a Rigid Body Motion, the two problems have the same incremental solution $(\Delta\boldsymbol{\epsilon}^p, \Delta\boldsymbol{\alpha}, \Delta\boldsymbol{\sigma})$, and therefore the Cauchy Problem is solved with $\Delta\mathbf{u}_1$, whereas the solution to the data completion problem is the pair $(\Delta\mathbf{u}_1, \Delta\boldsymbol{\eta})$ on Γ_u. A general variational method can thus be derived by building an error functional $\mathcal{E}$ between $\Delta e_1 = (\Delta\mathbf{u}_1, \Delta\boldsymbol{\epsilon}_1^p, \Delta\boldsymbol{\alpha}_1, \Delta\boldsymbol{\sigma}_1)$ and $\Delta e_2 = (\Delta\mathbf{u}_2, \Delta\boldsymbol{\epsilon}_2^p, \Delta\boldsymbol{\alpha}_2, \Delta\boldsymbol{\sigma}_2)$ as a function of $\Delta\boldsymbol{\eta}$ and by minimising it over all the possible surface traction fields defined on Γ_u.

$$\min_{\Delta\eta} \mathcal{J}(\Delta\boldsymbol{\eta}) \equiv \int_\Omega \mathcal{E}\left(\Delta e_1(\Delta\boldsymbol{\eta}), \Delta e_2(\Delta\boldsymbol{\eta})\right) \mathrm{d}\Omega \tag{7}$$

The next part is devoted to the derivation of various possible errors $\mathcal{E}$.

4. Errors in constitutive equations

The errors rely on the convexity property of the free energy and dissipation potential, by using the following lemma:

Lemma 4.1. *Let $f(x)$ be a real nonlinear convex lsc function on $\mathbb{R}^n$. If $f(x)$ and its convex conjugate $f^*(x)$ are truly nonlinear, then for any quadruplet (x_1, y_1, x_2, y_2) such that $y_1 \in \partial f(x_1)$, $y_2 \in \partial f(x_2)$, one has:*

(i) $(y_1 - y_2) \cdot (x_1 - x_2) \geq 0$
(ii) $(y_1 - y_2) \cdot (x_1 - x_2) = 0 \Leftrightarrow x_1 = x_2$ *and* $y_1 = y_2$

Proof. The proof is straightforward when using the Legendre–Fenchel inequality in Ekeland and Temam [33] involving the conjugate function f^* of the function f:

$$\begin{cases} f(x) + f^*(y) - x.y \geq 0 \quad \forall x, y \\ f(x) + f^*(y) - x.y = 0 \;\Leftrightarrow\; y \in \partial f(x) \Leftrightarrow\; x \in \partial f^*(y) \end{cases}$$

Indeed, the inequality (i) is obtained by summing the Fenchel inequalities for (x_1, y_2) and (x_2, y_1) and the Fenchel equalities for (x_1, y_1) and (x_2, y_2). Always using the identity of the right-hand side of (i) with the sum of Fenchel (positive) inequalities, it is easy to see that vanishing of (i) is equivalent to

$$y_1 \in \partial f(x_2) \text{ and } y_2 \in \partial f(x_1)$$

Let take the first result and use the definition of the sub-differential at x_2 and at x_1 with y_1:

$$\left.\begin{array}{l} f(x) - f(x_2) \geq y_1 \cdot (x - x_2) \\ f(x) - f(x_1) \geq y_1 \cdot (x - x_1) \end{array}\right\} \Rightarrow f(x_1) - f(x_2) \geq y_1 \cdot (x_1 - x_2) \geq f(x_1) - f(x_2)$$

so that if f is truly nonlinear, one must have $x_2 = x_1$. By the same reasoning, interchanging the dual quantities x and y, and using the conjugate function f^*, one gets $y_2 = y_1$. □

Owing to the general form of the constitutive equation, we can then derive errors with suitable properties. They are positive quantities and whenever they vanish then the distance between the two state variable increments vanishes together with the distance of their dual counterparts.

$$\mathcal{E}_W(\Delta\boldsymbol{\sigma}_1, \Delta\boldsymbol{\epsilon}_1; \Delta\boldsymbol{\sigma}_2, \Delta\boldsymbol{\epsilon}_2) = (\Delta\boldsymbol{\sigma}_1 - \Delta\boldsymbol{\sigma}_2) : (\Delta\boldsymbol{\epsilon}_1^{\mathrm{e}} - \Delta\boldsymbol{\epsilon}_2^{\mathrm{e}}) - (\mathbf{A}_1 - \mathbf{A}_2) \cdot (\Delta\boldsymbol{\alpha}_1 - \Delta\boldsymbol{\alpha}_2) \tag{8}$$

$$\mathcal{E}_\Psi(\Delta\boldsymbol{\sigma}_1, \Delta\boldsymbol{\epsilon}_1^{\mathrm{p}}; \Delta\boldsymbol{\sigma}_2, \Delta\boldsymbol{\epsilon}_2^{\mathrm{p}}) = (\Delta\boldsymbol{\sigma}_1 - \Delta\boldsymbol{\sigma}_2) : (\Delta\boldsymbol{\epsilon}_1^{\mathrm{p}} - \Delta\boldsymbol{\epsilon}_2^{\mathrm{p}}) + (\mathbf{A}_1 - \mathbf{A}_2) \cdot (\Delta\boldsymbol{\alpha}_1 - \Delta\boldsymbol{\alpha}_2) \tag{9}$$

The first error is naturally called error in free energy, whereas the second one is called error in dissipation. They can be combined in order to define a general function via a parameter $0 \leq \chi \leq 1$, as shown in a different framework by Hadj Sassi and Andrieux [34].

$$\mathcal{E}_\chi = (1-\chi)\,\mathcal{E}_W + \chi\,\mathcal{E}_\psi \tag{10}$$

The previous error are recovered for extreme values of the parameter χ. The parameterisation allows one to put different weights on the errors in stored energy and dissipated energy, but outstandingly the mean value of the parameter ($\chi = 1/2$) that makes free energy error and dissipated energy error exactly balance leads, to what can be called the Drücker error [35]:

$$\mathcal{E}_{\frac{1}{2}} = \frac{1}{2}(\Delta\boldsymbol{\sigma}_1 - \Delta\boldsymbol{\sigma}_2) : (\Delta\boldsymbol{\epsilon}_1 - \Delta\boldsymbol{\epsilon}_2) \tag{11}$$

Remark 1. Due to Lemma 4.1, the extreme value $\chi = 1$ corresponding to a pure dissipative error function must be discarded because the 1-homogeneous potential of dissipation Ψ is not truly nonlinear.

The Drücker error is an error in total mechanical energy; for the elastoplastic situation let us give more details about the previously defined error.

- Perfect elastoplastic material: $W(\boldsymbol{\epsilon}, \boldsymbol{\epsilon}^{\mathrm{p}}) = \frac{1}{2}(\boldsymbol{\epsilon} - \boldsymbol{\epsilon}^{\mathrm{p}}) : \mathbb{C} : (\boldsymbol{\epsilon} - \boldsymbol{\epsilon}^{\mathrm{p}})$, where $\boldsymbol{\epsilon} - \boldsymbol{\epsilon}^{\mathrm{p}} = \boldsymbol{\epsilon}^{\mathrm{e}}$ is the elastic strain tensor and $\boldsymbol{\epsilon}^{\mathrm{p}} : \boldsymbol{I} = 0$ and $\Psi(\dot{\boldsymbol{\epsilon}}^{\mathrm{p}}) = \sigma_0 \|\dot{\boldsymbol{\epsilon}}^{\mathrm{p}}\| \cdot \sigma_0$ and $\mathbb{C}$ denote the yielding stress and the Hooke tensor, respectively. The yield function is $f(\boldsymbol{\sigma}) = \sigma_{\mathrm{eq}} - \sigma_0$, where σ_{eq} is the von Mises stress. Therefore, the error functional is:

$$\mathcal{E}_\chi = (1-\chi)\,(\Delta\boldsymbol{\sigma}_1 - \Delta\boldsymbol{\sigma}_2) : (\Delta\boldsymbol{\epsilon}_1^{\mathrm{e}} - \Delta\boldsymbol{\epsilon}_2^{\mathrm{e}}) + \chi\,(\Delta\boldsymbol{\sigma}_1 - \Delta\boldsymbol{\sigma}_2) : (\Delta\boldsymbol{\epsilon}_1^{\mathrm{p}} - \Delta\boldsymbol{\epsilon}_2^{\mathrm{p}}) \tag{12}$$

- Elastoplastic material with isotropic hardening: the hardening function is defined by $R(\gamma) = -H\gamma + \sigma_0$, where γ is the accumulated plastic strain, so $\boldsymbol{\alpha} = \gamma$ and $A = -H\gamma$ and the free energy is defined by:

$$W(\boldsymbol{\epsilon}, \boldsymbol{\epsilon}^{\mathrm{p}}, \boldsymbol{\alpha}) = \frac{1}{2}(\boldsymbol{\epsilon} - \boldsymbol{\epsilon}^{\mathrm{p}}) : \mathbb{C} : (\boldsymbol{\epsilon} - \boldsymbol{\epsilon}^{\mathrm{p}}) + \int_0^{\boldsymbol{\alpha}} (R(\boldsymbol{\beta}) - \sigma_0)\,\mathrm{d}\boldsymbol{\beta} \tag{13}$$

and $\Psi(\dot{\boldsymbol{\epsilon}}^{\mathrm{p}}, \dot{\boldsymbol{\alpha}}) = \sigma_0 \|\dot{\boldsymbol{\epsilon}}^{\mathrm{p}}\| + \mathbb{I}_{\dot{\boldsymbol{\alpha}} = \sqrt{2/3}\|\dot{\boldsymbol{\epsilon}}^{\mathrm{p}}\|}$ and the yield function is $f(\boldsymbol{\sigma}, \boldsymbol{A}) = \sigma_{\mathrm{eq}} + A - \sigma_0$. The functional is then:

$$\begin{aligned}\mathcal{E}_\chi = {} & (1-\chi)\left[(\Delta\boldsymbol{\sigma}_1 - \Delta\boldsymbol{\sigma}_2) : (\Delta\boldsymbol{\epsilon}_1^{\mathrm{e}} - \Delta\boldsymbol{\epsilon}_2^{\mathrm{e}}) - \big(R(\boldsymbol{\alpha} + \Delta\boldsymbol{\alpha}_1) - R(\boldsymbol{\alpha} + \Delta\boldsymbol{\alpha}_2)\big) \cdot (\Delta\boldsymbol{\alpha}_1 - \Delta\boldsymbol{\alpha}_2)\right] \\ & + \chi\left[(\Delta\boldsymbol{\sigma}_1 - \Delta\boldsymbol{\sigma}_2) : (\Delta\boldsymbol{\epsilon}_1^{\mathrm{p}} - \Delta\boldsymbol{\epsilon}_2^{\mathrm{p}}) + \big(R(\boldsymbol{\alpha} + \Delta\boldsymbol{\alpha}_1) - R(\boldsymbol{\alpha} + \Delta\boldsymbol{\alpha}_2)\big) \cdot (\Delta\boldsymbol{\alpha}_1 - \Delta\boldsymbol{\alpha}_2)\right]\end{aligned} \tag{14}$$

Equipped with this error in energy functional, which can be also called error in constitutive equations, we can then define the general error functional to be minimised in order to get the solution to the data completion problem:

$$\mathcal{J}_\chi(\Delta\boldsymbol{\eta}) = \int_\Omega \mathcal{E}_\chi(\Delta e_1(\Delta\boldsymbol{\eta})), \Delta e_2(\Delta\boldsymbol{\eta}))\,\mathrm{d}\Omega \tag{15}$$

The Drücker error is the only one that can be computed by boundary integration on the whole external surface of the body, thanks to the virtual power principle. This feature has been largely exploited previously to improve the global performance of the solution algorithm for linear Cauchy Problem by Baranger and Andrieux [15].

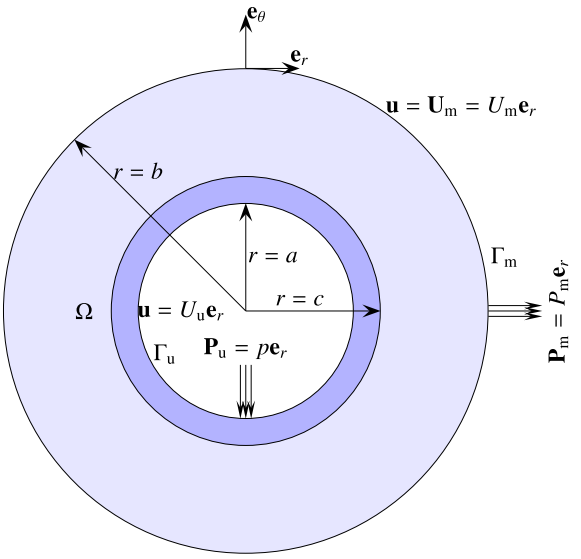

Fig. 1. (Colour online.) A spherical reservoir with inner radius a and outer radius b respectively ($a < b$). The inaccessible boundary Γ_u is at $r = a$.

5. A simple illustration: spherical reservoir

The illustration is conducted in order to examine the influence, in relative merits, of various energy errors, corresponding to various values of the parameter χ when used to build the function $\mathcal{J}_\chi(\Delta\boldsymbol{\eta})$. Even if in this very simple case, they turn out to be very similar. But the aim is also to analyse the precision of the reconstruction of the internal pressure and quantities inside the solid, especially for the plastic strain field, the position of the plastic zone, and the residual stress field at the end of the loading–unloading sequence. Due to the low dimension of the unknowns space, the general robustness of the method with respect to noisy data cannot be assessed here.

The solution method (7) is illustrated through the simple example of a pressurised spherical reservoir, on the external surface Γ_m of which the pressure and radial displacement increment histories are given (Fig. 1). The internal surface here is the boundary part Γ_u, where no data are available, and the arguments of the functional $\mathcal{J}_\chi$ in (7) reduce to the scalar internal incremental pressure denoted by Δp.

Thanks to the symmetry of the problem, closed-form solutions can be derived for the incremental problems $(\mathcal{P}_1)$ and $(\mathcal{P}_2)$ so that the function $\mathcal{J}_\chi$ turns out to have also a closed-form expression in the case of perfect and isotropic linear hardening elastoplasticity. Denoting by $\mathbf{n}$ the unit outer normal vector, the following incremental well-posed problems are derived by exploiting independently the Cauchy data U_m and P_m as in (5) and (6),

$$(\mathcal{P}_1)\begin{cases} \nabla\cdot\Delta\boldsymbol{\sigma}_1 = 0 & \text{in} \quad \Omega \\ \Delta\mathbf{u}_1 = \Delta U_\mathrm{m}\mathbf{e}_r & \text{on} \quad r=b \\ \Delta\boldsymbol{\sigma}_1\cdot\mathbf{n} = \Delta p\,\mathbf{e}_r & \text{on} \quad r=a \end{cases} \quad \text{and} \quad (\mathcal{P}_2)\begin{cases} \nabla\cdot\Delta\boldsymbol{\sigma}_2 = 0 & \text{in} \quad \Omega \\ \Delta\boldsymbol{\sigma}_2\cdot\mathbf{n} = \Delta P_\mathrm{m}\,\mathbf{e}_r & \text{on} \quad r=b \\ \Delta\boldsymbol{\sigma}_2\cdot\mathbf{n} = \Delta p\,\mathbf{e}_r & \text{on} \quad r=a \end{cases} \tag{16}$$

5.1. Closed-form solutions

To derive the solution to the incremental problems (16), given the increments Δp, ΔU_m and ΔP_m, two situations must be considered, namely pure elastic incremental response or elastoplastic increment with evolution of the plastic zone.

First, solutions of the continuous evolution problems will be derived in closed forms. Due to symmetry, the plastic zone reduces to a circular annulus with internal radius a and external radius, which will be denoted by c_i. The reservoir having a small thickness-to-mean-radius ratio, the radius of the plastic zone c is assumed to have a monotonic evolution law from $r = a$ (when internal pressure reaches the elastic limit pressure) to the extreme value c_max during the loading–unloading sequence. The material is characterised by the Lamé coefficients λ and μ, the yield stress σ_0 and the strain-hardening modulus H characterising a linear isotropic hardening. Closed form solutions for the elastic behaviour are:

$$u_r^i = C_i r + \frac{D_i}{r^2}, \quad \epsilon_r^i = C_i - \frac{2D_i}{r^3}, \quad \epsilon_\theta^i = \epsilon_\varphi^i = C_i + \frac{D_i}{r^3}, \quad i = 1,2 \tag{17}$$

$$\sigma_r^i = \mathcal{K}C_i - 4\mu\frac{D_i}{r^3}, \quad \sigma_\theta^i = \sigma_\varphi^i = \mathcal{K}C_i + 2\mu\frac{D_i}{r^3}, \quad i = 1,2 \tag{18}$$

where C_i and D_i are integral constants and $\mathcal{K} = 3\lambda + 2\mu$. The coefficients C_i and D_i are identified by using the following boundary conditions.

In the case of pure elastic behaviour, $a \le r \le b$: for the first problem $\sigma_r^1(r=a) = -p$ and $u_r^1(r=b) = U_\mathrm{m}$, for the second problem $\sigma_r^2(r=a) = -p$ and $\sigma_r^2(r=b) = P_\mathrm{m}$.

$$C_1 = \frac{4\,U_\mathrm{m}\,b^2\mu - a^3 p}{\kappa\,a^3 + 4\,b^3\mu},\ D_1 = \frac{\left(\kappa\,U_\mathrm{m}\,b^2 + b^3 p\right)a^3}{\kappa\,a^3 + 4\,b^3\mu} \quad \text{and} \quad C_2 = -\frac{P_\mathrm{m}\,b^3 + a^3 p}{\mathcal{K}\left(a^3 - b^3\right)},\ D_2 = -\frac{1}{4}\frac{(P_\mathrm{m} + p)\,b^3 a^3}{\left(a^3 - b^3\right)\mu} \tag{19}$$

In the case of elastoplastic behaviour, it occurs for $c_i \le r \le b$ with $i = 1, 2$: for the first problem, $\sigma_{\mathrm{eq}}^1(r = c_1) = \sigma_0$ and $u_r^1(r=b) = U_\mathrm{m}$; for the second problem, $\sigma_{\mathrm{eq}}^2(r = c_2) = \sigma_0$ and $\sigma_r^2(r=b) = P_\mathrm{m}$.

$$C_1 = -\frac{\sigma_Y\,{c_1}^3}{6\mu\,b^3} + \frac{U_\mathrm{m}}{b},\ D_1 = \frac{\sigma_Y\,{c_1}^3}{6\mu} \quad \text{and} \quad C_2 = \frac{2\sigma_0 {c_2}^3}{3\mathcal{K}b^3} + \frac{P_\mathrm{m}}{\mathcal{K}},\ D_2 = \frac{\sigma_0\,{c_2}^3}{6\mu} \tag{20}$$

The plastic solutions given hereafter for linear isotropic hardening correspond to $R(\beta) = H\gamma$ in (13), where γ is the accumulated plasticity strain. Thus for $a \le r \le c_i$ and $i = 1, 2$:

$$u_r^1 = \frac{2B}{3\mathcal{K}} r\left(3\ln(\frac{r}{c_1}) + \frac{{c_1}^3}{r^3} - 1\right) + \frac{\sigma_0}{6\mu} c_1^3 r\left(\frac{1}{r^3} - \frac{1}{b^3}\right) + \frac{U_\mathrm{m}}{b} r \tag{21}$$

$$\sigma_r^1 = \frac{2B}{3}\left(3\ln(\frac{r}{c_1}) + \frac{c_1^3}{r^3} - 1\right) - \frac{2\sigma_0}{3}{c_1}^3\left(\frac{1}{r^3} + \frac{\mathcal{K}}{4\mu b^3}\right) + \frac{\mathcal{K}\,U_\mathrm{m}}{b} \tag{22}$$

$$\sigma_\theta^1 = \frac{B}{3}\left(6\ln(\frac{r}{c_1}) - \frac{{c_1}^3}{r^3} + 1\right) + \frac{\sigma_0}{3} c_1^3\left(\frac{1}{r^3} - \frac{\mathcal{K}}{2\mu b^3}\right) + \frac{\mathcal{K} U_\mathrm{m}}{b} \tag{23}$$

$$u_r^2 = \frac{2B}{3\mathcal{K}} r\left(3\ln(\frac{r}{c_2}) + \frac{{c_2}^3}{r^3} - 1\right) + \frac{2\sigma_0}{3\mathcal{K}} {c_2}^3 r\left(\frac{1}{b^3} + \frac{\mathcal{K}}{4\mu r^3}\right) + \frac{P_\mathrm{m}}{\mathcal{K}} r \tag{24}$$

$$\sigma_r^2 = \frac{2B}{3}\left(3\ln(\frac{r}{c_2}) + \frac{{c_2}^3}{r^3} - 1\right) + \frac{2\sigma_0}{3}{c_2}^3\left(\frac{1}{b^3} - \frac{1}{r^3}\right) + P_\mathrm{m} \tag{25}$$

$$\sigma_\theta^2 = \frac{B}{3}\left(6\ln(\frac{r}{c_2}) - \frac{{c_2}^3}{r^3} + 1\right) + \frac{2\sigma_0}{3} c_2^3\left(\frac{1}{b^3} + \frac{1}{2r^3}\right) + P_\mathrm{m} \tag{26}$$

and the transcendental equations for the elastoplastic boundary c_i, with $i = 1, 2$, in terms of the inner pressure p are:

$$p = \frac{2B}{3}\left(3\ln\left(\frac{c_1}{a}\right) - \frac{{c_1}^3}{a^3} + 1\right) + \frac{2\sigma_0}{3}\frac{{c_1}^3}{a^3}\left(1 + \frac{\mathcal{K}a^3}{4\mu b^3}\right) - \frac{\mathcal{K}\,U_\mathrm{m}}{b} \tag{27}$$

$$p = \frac{2B}{3}\left(3\ln(\frac{c_2}{a}) - \frac{{c_2}^3}{a^3} + 1\right) + \frac{2\sigma_0}{3}\frac{{c_2}^3}{a^3}\left(1 - \frac{a^3}{b^3}\right) - P_\mathrm{m} \tag{28}$$

where B is a constant depending on Lamé parameters λ and μ, yield stress σ_0 and the H the strain-hardening modulus:

$$B = \frac{3\mathcal{K}\mu\,\sigma_0}{\mathcal{K}H + 3\mathcal{K}\mu + 4H\mu}$$

Notice that when $B = \sigma_0$ for the particular value of $H = 0$, we obtain the closed form solution for perfect plastic material. The accumulated plastic strain function $\gamma_i(r)$ and the Von Mises criterion σ_{eq} are:

$$\gamma_i(r) = \frac{\sigma_{\mathrm{eq}} - \sigma_0}{H} = B + \frac{(\sigma_0 - B)}{H}\left(\frac{c_i^3}{r^3} - 1\right) \quad \text{for} \quad i = 1, 2 \tag{29}$$

$$\sigma_{\mathrm{eq}} = \sigma_\theta^i - \sigma_r^i = B + (\sigma_0 - B)\frac{c_i^3}{r^3} \quad \text{for} \quad i = 1, 2 \tag{30}$$

Using the above solutions, incremental quantities can be derived in order to solve the incremental problems defined by (16).

Incremental elastic evolution In this case, the solution to the incremental evolution problem, for the displacement increment, the stress increment and the total strain increment have the above forms (the incremental plastic strain is zero), and the coefficients C_i and D_i are identified and updated by using the boundary condition of each problem at each loading/unloading increment by the following quantities:

$$\begin{cases} \Delta C_1 = \dfrac{4\mu(b^2/a^3)\Delta U_{\rm m} - \Delta p}{\mathcal{K} + 4\mu(b/a)^3} \\ \Delta D_1 = \dfrac{\mathcal{K}b^2\Delta U_{\rm m} + b^3\Delta p}{\mathcal{K} + 4\mu(b/a)^3} \end{cases} \quad \text{and} \quad \begin{cases} \Delta C_2 = \dfrac{\Delta P_{\rm m} b^3 + a^3\Delta p}{\mathcal{K}(b^3 - a^3)} \\ \Delta D_2 = \dfrac{(\Delta P_{\rm m} + \Delta p)(ab)^3}{4\mu(b^3 - a^3)} \end{cases} \tag{31}$$

The solution given by (17) and (18) must be checked with respect to the yield criterion $f(\boldsymbol{\sigma}, \boldsymbol{\alpha}) < 0$. If the criterion is not satisfied somewhere inside the domain (generally in the vicinity of the plastic zone limit $r = c$ or near the internal boundary $r = a$), then this elastic trial must be rejected and one has to turn towards the elastoplastic case.

Incremental elastoplastic evolution Assuming the symmetry is preserved in this incremental evolution, the unknowns are supplemented with the incremental plastic zone radius ($\Delta c_i > 0$) and the plastic strain increment field. The evolution equations are supplemented with the yield limit equation $f(\boldsymbol{\sigma} + \Delta\boldsymbol{\sigma}, \boldsymbol{A} + \Delta\boldsymbol{A}) = 0$ within the (unknown) plastic zone, and the continuity conditions at $r = c_i + \Delta c_i$, for $i = 1, 2$. The plasticity phenomenon considered here includes perfect plasticity and isotropic hardening plasticity.

1. Consider the *isotropic linear hardening behaviour*, the incremental quantities Δc_1 and Δc_2 are related to the incremental quantities Δp, $\Delta U_{\rm m}$ and $\Delta P_{\rm m}$ via the following equations,

$$\frac{\Delta p}{2B} + \frac{\mathcal{K}\Delta U_{\rm m}}{2bB} = \ln\left(1 + \frac{\Delta c_1}{c_1}\right) + \frac{1}{3}\frac{c_1^3}{a^3}\left[1 - \frac{\sigma_0}{B}\left(1 + \frac{\mathcal{K}}{4\mu}\frac{a^3}{b^3}\right)\right]\left(1 - \left(1 + \frac{\Delta c_1}{c_1}\right)^3\right) \tag{32}$$

$$\frac{\Delta p}{2B} + \frac{\Delta P_{\rm m}}{2B} = \ln\left(1 + \frac{\Delta c_2}{c_2}\right) + \frac{1}{3}\frac{c_2^3}{a^3}\left[1 - \frac{\sigma_0}{B}\left(1 - \frac{a^3}{b^3}\right)\right]\left(1 - \left(1 + \frac{\Delta c_2}{c_2}\right)^3\right) \tag{33}$$

when Δc_1 and Δc_2 are computed, it is straightforward to compute the incremental quantities ΔC_i and ΔD_i for $i = 1, 2$ by using the corresponding equations (20).

$$\begin{cases} \Delta C_1 = \dfrac{\Delta U_{\rm m}}{b} + \dfrac{\sigma_0 c_1^3}{6\mu b^3}\left[1 - \left(1 + \dfrac{\Delta c_1}{c_1}\right)^3\right] \\ \Delta D_1 = -\dfrac{\sigma_0 c_1^3}{6\mu}\left[1 - \left(1 + \dfrac{\Delta c_1}{c_1}\right)^3\right] \end{cases} \quad \text{and} \quad \begin{cases} \Delta C_2 = \dfrac{\Delta P_{\rm m}}{\mathcal{K}} - \dfrac{2\sigma_0 c_2^3}{3\mathcal{K}b^3}\left[1 - \left(1 + \dfrac{\Delta c_2}{c_2}\right)^3\right] \\ \Delta D_2 = -\dfrac{\sigma_0 c_2^3}{6\mu}\left[1 - \left(1 + \dfrac{\Delta c_2}{c_2}\right)^3\right] \end{cases} \tag{34}$$

2. Consider the *perfect plastic behaviour* characterised by the yielding stress σ_0 and $H = 0$, the incremental quantities are obtained by taking $B = \sigma_0$ in the above equations.

The function $\mathcal{J}_\chi(\Delta p)$ can be computed in closed form, and for instance the Drücker error function is simply:

$$\mathcal{J}_{\frac{1}{2}}(\Delta p) = 2\pi b\left(\mathcal{K}\Delta C_1 - 4\mu\frac{\Delta D_1}{b^3} - \Delta P_{\rm m}\right)\left(\Delta U_{\rm m} - \Delta C_2 b - \frac{\Delta D_2}{b^2}\right) \tag{35}$$

Notice that only the part of the integral on $\Gamma_{\rm m}$ appears in the above expression, the part corresponding to the integral on $\Gamma_{\rm u}$ vanishes because problems $\mathcal{P}_1$ and $\mathcal{P}_2$ in (16) have the same boundary condition on $\Gamma_{\rm u}$ (see Baranger and Andrieux [15] for other possibilities).

Remark 2. If the over-specified data $U_{\rm m}$ and $P_{\rm m}$ are compatible, they are related to the inner pressure p by the following relations:

- in the case of a pure elastic behaviour:

$$P_{\rm m} = \frac{4\mu\mathcal{K}(b^3 - a^3)}{(a^3\mathcal{K} + 4b^3\mu)b}U_{\rm m} - \frac{a^3 b(\mathcal{K} + 4\mu)}{(a^3\mathcal{K} + 4b^3\mu)b}p$$

- in the case of an elastoplastic behaviour, the interfaces verify $c_1 = c_2 = c$ and

$$\frac{\mathcal{K}}{b}U_{\rm m} - P_{\rm m} = \frac{2\sigma_0}{3}\frac{c^3}{b^3}\left(1 + \frac{\mathcal{K}}{4\mu}\right)$$

5.2. Numerical experiments

This section is devoted to numerical experiments. The internal and external radiuses are: $a = 400$ mm and $b = 600$ mm. The material parameters are: Young modulus $E = 210\,000$ MPa (Young modulus), Poisson ratio $\nu = 1/3$, yield stress

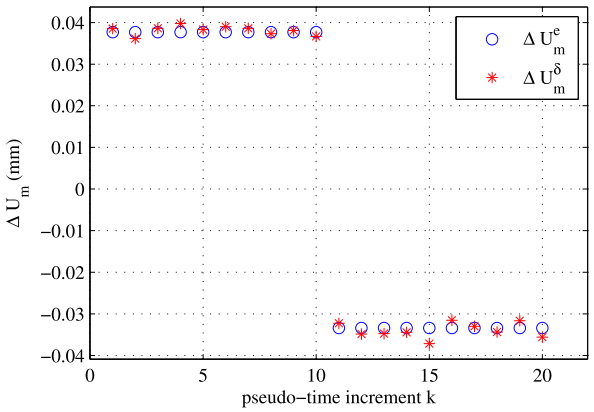

(a) Noise-free and noisy Cauchy data (10%).

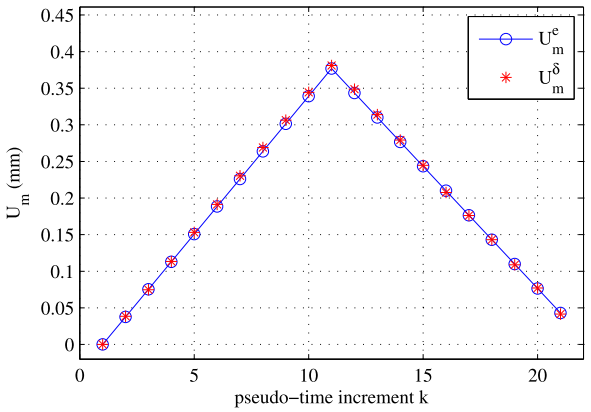

(b) Noise-free and noisy Cauchy data (10%).

Fig. 2. (Colour online.) Exact and noisy radial displacement U_{m}^k and increment ΔU_{m}^k at each pseudo increment time k. "e" denotes exact data, k denotes the increment number and δ denotes noisy data.

$\sigma_0 = 400$ MPa and the tangent modulus $E_T = 0.1E = 21\,000$ MPa. Without loss off generality, P_{m} (external pressure) is taken equal to zero. Therefore all above materials parameters are: $\lambda = 15\,325$ MPa, $\mu = 78\,947$ MPa, $\mathcal{K} = 61\,765$ MPa, $H = 23\,333$ MPa, and $B = 348.1625$ MPa.

The reference solution U_{m} is the following for an internal pressure p-history going from zero, reaching the maximal value $p^{\max}$ and going back to zero:

$$\begin{cases} \text{elastic loading:} \\ 0 < p < p_a = \dfrac{2\sigma_0}{3}\dfrac{b^3 - a^3}{b^3} = 187.6543 \text{ MPa} \quad \Rightarrow \quad 0 \le U_{\mathrm{m}} < U_{\mathrm{m}a} = \dfrac{2a}{3}\sigma_0\left(\dfrac{a^3}{\mathcal{K}b^3} + \dfrac{1}{4\mu}\right) = 0.2269 \text{ mm} \quad \text{(a)} \\ \text{elastoplastic loading:} \\ p_a \le p < p^{\max} = 276.0329 \text{ MPa} < p_b = \dfrac{2}{3}\left(3\ln\left(\dfrac{b}{a}\right) + (1 - \dfrac{b^3}{a^3})(B - \sigma_0)\right) = 364.4116 \text{ MPa} \\ \quad \text{and } \dfrac{\mathrm{d}p}{\mathrm{d}t} > 0 \quad \Rightarrow \quad U_{\mathrm{m}}^{\max} = 0.3768 \text{ mm} < U_{\mathrm{m}b} = \dfrac{2\sigma_0 b}{3}\left(\dfrac{1}{\mathcal{K}} + \dfrac{1}{4\mu}\right) = 0.7657 \text{ mm} \quad \text{(b)} \\ \text{elastic unloading:} \\ 0 < p < p^{\max} \text{ and } \dfrac{\mathrm{d}p}{\mathrm{d}t} < 0 \quad \Rightarrow \quad U_{\mathrm{m}}^{\text{residual}} = U_{\mathrm{m}}^{\max} - p^{\max}\dfrac{a^3 b}{b^3 - a^3}\left(\dfrac{1}{\mathcal{K}} + \dfrac{1}{4\mu}\right) = 0.0431 \text{ mm} \quad \text{(c)} \end{cases} \tag{36}$$

where the pairs $(p_a, U_{\mathrm{m}a})$ and $(p_b, U_{\mathrm{m}b})$ are the inner pressures and the outer radial displacements when plasticity appears at internal boundary $c = a$ and when plasticity reaches the outer boundary $c = b$, corresponding to fully plastic linear strain-hardening state. The identification process of the internal pressure evolution is carried out by Algorithm 1.

Data: The domain Ω and its boundary $\partial\Omega = \Gamma_{\mathrm{m}} \cup \Gamma_{\mathrm{u}}$, the material parameters, the Cauchy data $(U_{\mathrm{m}}, P_{\mathrm{m}})$ on Γ_{m} and a given number of pseudo-time increments N_{incr};
Result: Pressure evolution on Γ_u;
initialisation: $k = 1$, $p^0 = 0$, P_{m}^0, U_{m}^0, $\Delta p^k = 0$, ΔP_{m}^k and ΔU_{m}^k;
while $k \le N_{\mathrm{incr}}$ **do**
Solve the following minimisation problem:

$$\Delta p^k = \arg\min_{\Delta p} \mathcal{J}(\Delta p; \Delta U_{\mathrm{m}}^k, \Delta P_{\mathrm{m}}^k), \quad J(\Delta p; \Delta U_{\mathrm{m}}^k, \Delta P_{\mathrm{m}}^k) \text{ is given by (35)}$$

$p^k = p^{k-1} + \Delta p^k$;
$P_{\mathrm{m}}^k = P_{\mathrm{m}}^{k-1} + \Delta P_{\mathrm{m}}^k$;
$U_{\mathrm{m}}^k = U_{\mathrm{m}}^{k-1} + \Delta U_{\mathrm{m}}^k$;
end

Algorithm 1: Incremental inner pressure identification.

Figs. 2a and 2b show respectively the exact and noisy displacement $U_{\mathrm{m}}^{\mathrm{e}}$ and U_{m}^{δ} and their increments $\Delta U_{\mathrm{m}}^{\mathrm{e}}$ and $\Delta U_{\mathrm{m}}^{\delta}$. The noisy displacement increments $\Delta U_{\mathrm{m}}^{\delta}$ are built by adding $\xi = 10\%$ of artificial Gaussian white noise:

$$\Delta U_{\mathrm{m}}^{\delta} = \Delta U_{\mathrm{m}} + \xi \max(\Delta U_{\mathrm{m}})\,\delta, \quad \delta \text{ is a Gaussian white noise vector with zero mean and unit variance.} \tag{37}$$

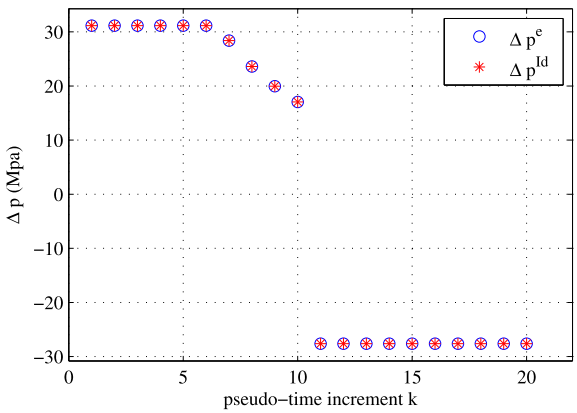

(a) Noise-free Cauchy data.

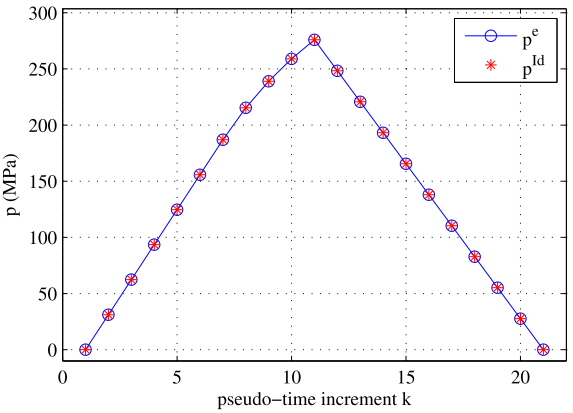

(b) Noise-free Cauchy data.

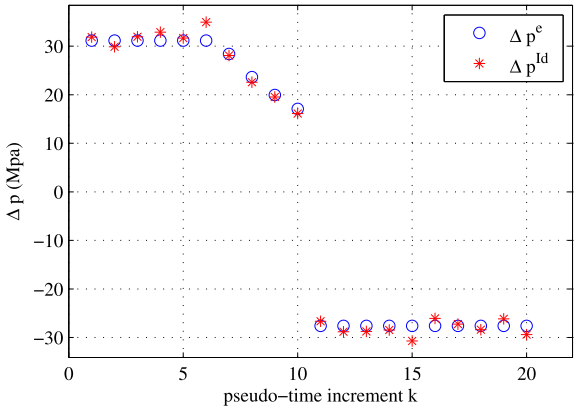

(c) Noisy Cauchy data (10%).

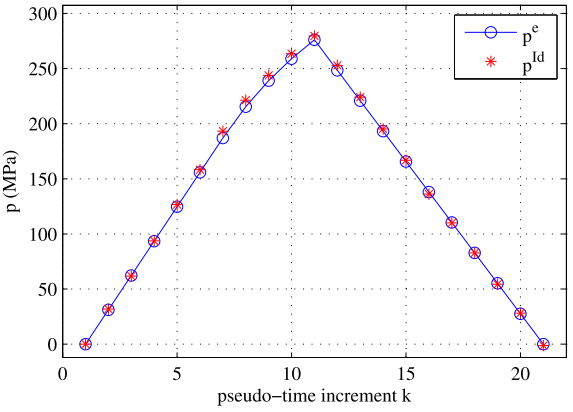

(d) Noisy Cauchy data (10%).

Fig. 3. (Colour online.) Exact and identified pressure increment Δp^k and its corresponding pressure p^k at each pseudo increment time k, obtained with noise-free and noisy Cauchy data. "e" denotes exact data, "id" denotes identified data, k denotes increment number and δ denotes noisy data.

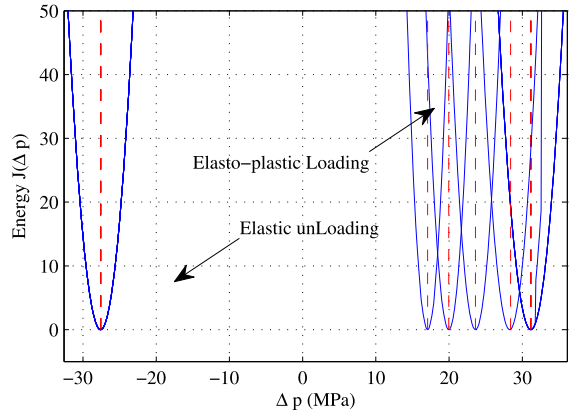

(a) Noise-free Cauchy data.

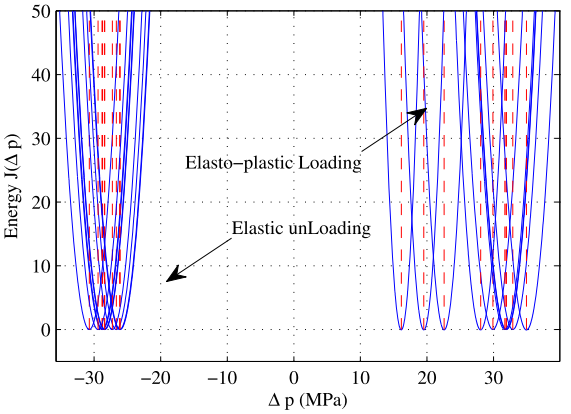

(b) Noisy Cauchy data (10%).

Fig. 4. (Colour online.) Error functional $\mathcal{J}_{\frac{1}{2}}(\Delta p)$ in the vicinity of each optimal increment Δp^k shown by the dashed line. k denotes the increment number.

Figs. 3a, 3b, 3c and 3d show the identified inner pressure increment Δp^k and its corresponding inner pressure p^k at each pseudo-time increment. Notice that there is a very good agreement with the exact values when the Cauchy data are noise free, and we observe some perturbations when the Cauchy data are noisy (10%). Nevertheless these results remain acceptable.

Fig. 4a shows the error function $\mathcal{J}(\Delta p)$ obtained with noise-free Cauchy data for each increment in the vicinity of the optimal value Δp^k (illustrated by the dashed red line), where k denotes the increment number, whereas Fig. 4b shows these

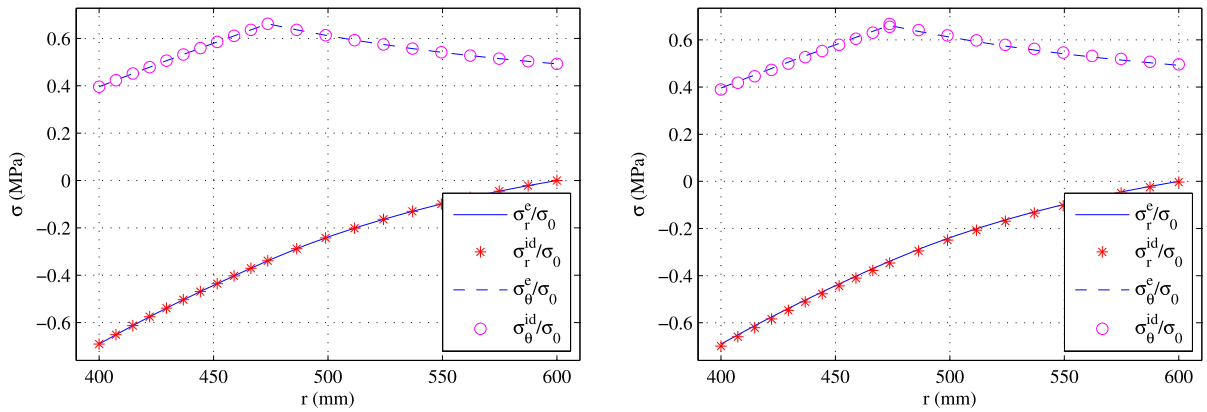

(a) Noise-free Cauchy data. (b) Noisy Cauchy data (10%).

Fig. 5. (Colour online.) Stress components σ_r and σ_θ identified with noise-free and noisy Cauchy data at the end of the loading path. "e" denotes exact data, "id" denotes identified data.

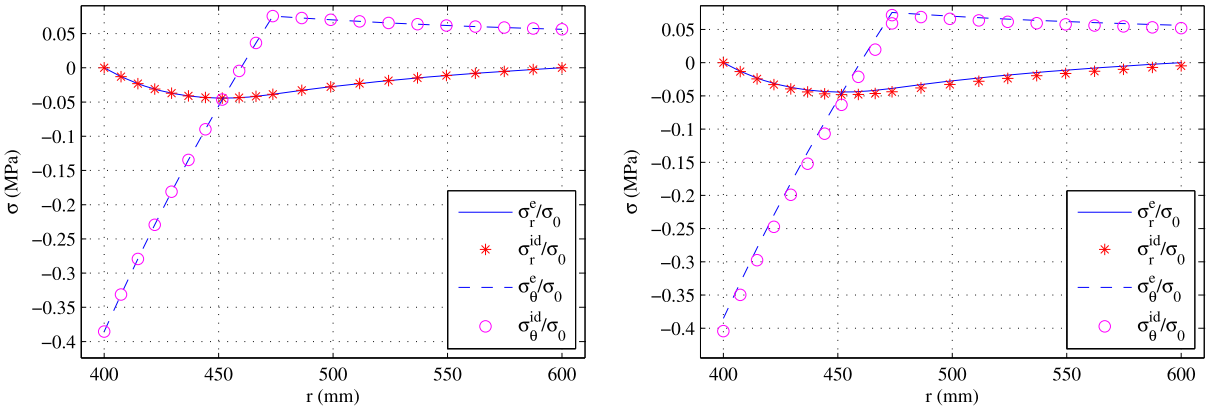

(a) Noise-free Cauchy data. (b) Noisy Cauchy data (10%).

Fig. 6. (Colour online.) Residual stress components σ_r and σ_θ identified with noise-free and noisy Cauchy data at the end of the unloading path. "e" denotes exact data, "id" denotes identified data.

functions obtained with noisy Cauchy data. Notice here that each function is shifted by noise effects, but remains convex and regular.

Normalised elastoplastic stresses at the end the loading path are plotted in Figs. 5a and 5b and normalised residual stresses upon depressurisation are shown in Figs. 6a and 6b. In the two cases, we observe a good agreement with the exact values, even when the Cauchy data are noisy. The accumulated plastic strain $\gamma(r)$ defined by (29) and identified with noise-free and noisy Cauchy data at the end of the loading path is shown in Figs. 7a and 7b. The elastoplastic interface radius c identified at each increment k is shown in Figs. 8a and 8b. We observe a good agreement with the exact values, except for the increment when the thick-walled spherical shell yields at the inner surface. Indeed, as the number of increment is chosen randomly, yielding may be achieved at the beginning, the end or inside an increment, so that the larger the increment is, the greater the error on the first yielding at the inner surface is. It is possible to improve this error after a first identification of the whole behaviour using large increments, by carrying out a second identification procedure using smaller increments at the zone where plasticity appears.

Fig. 9 shows the ratio of the relative errors of the identified inner incremental pressures Δp by each element of the noise vector δ used to generate noisy Cauchy data. Four different Gaussian white-noise vectors δ_i with zero mean and unit variance are used with the same noise level $\xi = 10\%$:

$$\mathcal{E}rror = \frac{\frac{|\Delta p^e - \Delta p^\delta|}{|\Delta p^e|}}{\delta} \tag{38}$$

We observe that the noise level of the Cauchy data and the identified pressure is constant, except in the transition zone when the plasticity appears. Indeed, in this example, the noise effect is linear during elastic loading and unloading phases, thus we observe a direct proportionality between the noisy data and the identified ones, whereas, in the elastoplastic

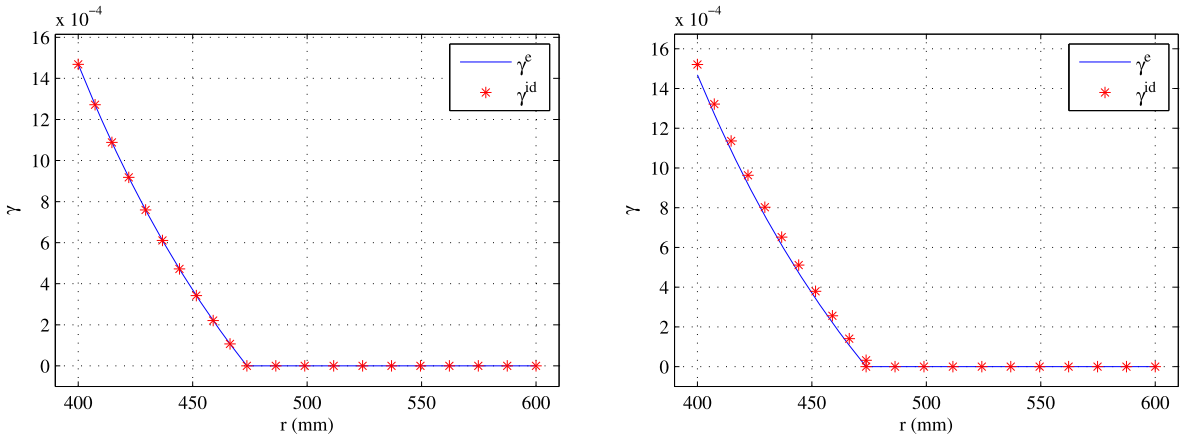

(a) Noise-free Cauchy data. (b) Noisy Cauchy data.

Fig. 7. (Colour online.) The cumulative plastic strain γ identified with noise-free and noisy Cauchy data at the end of the loading path. "e" denotes exact data, "id" denotes identified data.

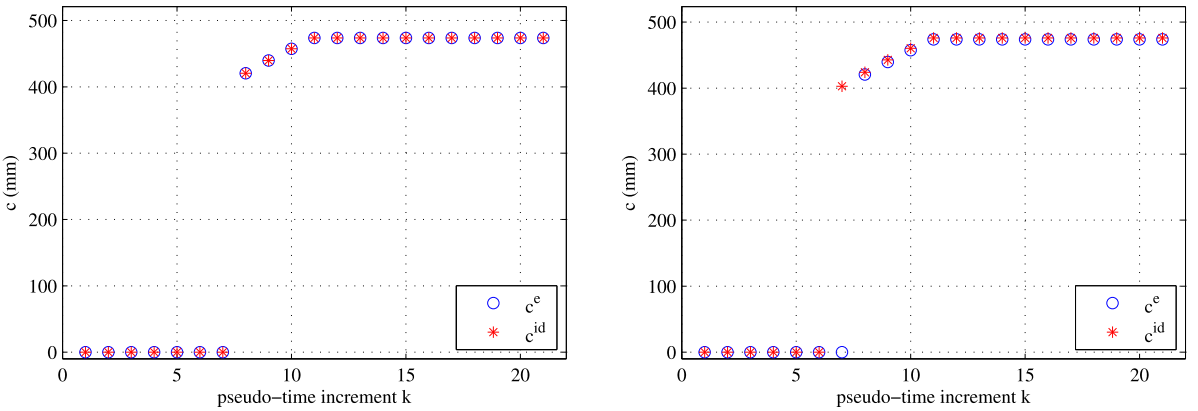

(a) Noise-free Cauchy data. (b) Noisy Cauchy data.

Fig. 8. (Colour online.) Elastoplastic interface c identified with noise-free and noisy Cauchy data at the end of the loading path. "e" denotes exact data, "id" denotes identified data.

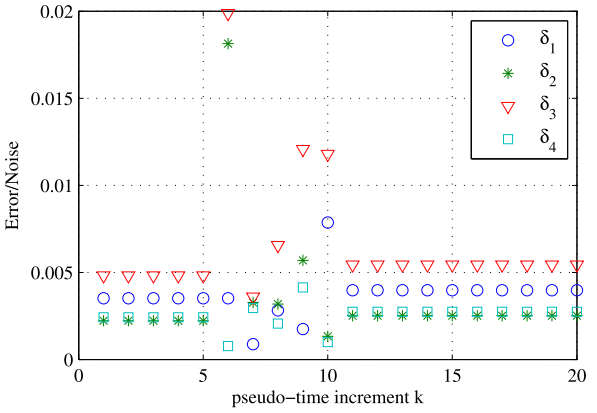

Fig. 9. (Colour online.) Ratio of the relative error of the identified pressure and the noise vector (38).

loading of transition, this effect is fully nonlinear, as shown in Fig. 9. A wise choice of the number of increments in each zone and of the regularisation techniques will allow us to improve these results.

6. Conclusions and perspectives

We derive a general method for the resolution of the Cauchy Problem for incremental elastic linear strain-hardening plasticity. Based on the splitting of the problem into two well-posed evolution problems, the derivation of a one-parameter family of energy errors, and the minimisation of it, the method has shown firstly that the loading–unloading phenomenon, which is very specific to elasto-plasticity can be dealt with, and secondly that the precision for the identification of unknown boundary data and of the plastic strain field is very good. Work under progress is devoted to numerical three-dimensional applications and evaluation of the effects of noise in the Cauchy data on the identifications' previsions. Potential applications include the identification of material parameters and residual stress states after the elaborating processes.

Acknowledgements

The authors wish to thank the Department AMA of EDF Research and Development Division (France) for its financial support (517-2013 Contrat N° 8610-4300365755EDF).

References

[1] H.D. Bui, Inverse Problems in the Mechanics of Materials: An Introduction, CRC Press, Boca Raton, FL, USA, 1994.
[2] H.D. Bui, Fracture Mechanics: Inverse Problems and Solutions, Springer, 2006.
[3] M. Bonnet, H.D. Bui, On some inverse problems for determining volumic defects by electric current using BIE approaches: an overview, in: Proceedings of the 6th National Japanese Conference on Boundary Elements Methods, Tokyo, Japan, 1989, pp. 179–198.
[4] Y.C. Hon, T. Wei, Backus–Gilbert algorithm for the Cauchy problem of the Laplace equation, Inverse Probl. 17 (2) (2001) 261.
[5] V.A. Kozlov, V.G. Maz'ya, A.F. Fomin, An iterative method for solving the Cauchy problem for elliptic equations, Comput. Math. Math. Phys. 31 (1992) 45–52.
[6] A. Cimetière, F. Delvare, M. Jaoua, F. Pons, Solution of the Cauchy problem using iterated Tikhonov regularisation, Inverse Probl. 17 (3) (2001) 553–570.
[7] R. Lattes, J.-L. Lions, Méthode de quasi-réversibilité et applications, Dunod, Paris, 1967.
[8] L. Bourgeois, Convergence rates for the quasi-reversibility method to solve the Cauchy problem for Laplace's equation, Inverse Probl. 22 (2) (2006) 413.
[9] L. Marin, D. Lesnic, Boundary element solution for the Cauchy problem in linear elasticity using singular value decomposition, Comput. Methods Appl. Mech. Eng. 191 (29–30) (2002) 3257–3270.
[10] L. Marin, D. Lesnic, The method of fundamental solutions for the Cauchy problem in two-dimensional linear elasticity, Int. J. Solids Struct. 41 (13) (2004) 3425–3438.
[11] C. Ghnatios, F. Chinesta, A. Leygue, P. Villon, P. Breitkopf, A. Poitou, Stratégies avancées d'optimisation et analyse inverse basées sur l'utilisation de la PGD, in: 10e Colloque National en Calcul des Structures, Gien, France, 2011.
[12] C. Stolz, Optimal control approach in nonlinear mechanics, C. R. Mecanique 336 (1–2) (2008) 238–244.
[13] P. Kugler, A. Leitão, Mean value iterations for nonlinear elliptic Cauchy problems, Numer. Math. 96 (2) (2003) 269–293.
[14] H. Egger, A. Leitão, Nonlinear regularisation methods for ill-posed problems with piecewise constant or strongly varying solutions, Inverse Probl. 25 (11) (2009) 115014.
[15] T.N. Baranger, S. Andrieux, Constitutive law gap functionals for solving the Cauchy problem for linear elliptic PDE, Appl. Math. Comput. 218 (5) (2011) 1970–1989.
[16] A. Leitão, An iterative method for solving elliptic Cauchy problems, Numer. Funct. Anal. Optim. 21 (2000) 715–742.
[17] L. Marin, The minimal error method for the Cauchy next term problem in linear elasticity. Numerical implementation for two-dimensional homogeneous isotropic linear elasticity, Int. J. Solids Struct. 46 (5) (2005) 957–974.
[18] T.N. Baranger, S. Andrieux, An optimization approach for the Cauchy problem in linear elasticity, Struct. Multidiscip. Optim. 35 (2) (2008) 141–152.
[19] S. Andrieux, T.N. Baranger, An energy error-based method for the resolution of the Cauchy problem in 3D linear elasticity, Comput. Methods Appl. Mech. Eng. 197 (2008) 902–920.
[20] T.N. Baranger, S. Andrieux, Data completion for linear symmetric operators as a Cauchy problem: an efficient method via energy like error minimisation, Vietnam J. Mech. 31 (2009) 247–261.
[21] S. Andrieux, T.N. Baranger, Emerging crack front identification from tangential surface displacements, C. R. Mecanique 340 (8) (2012) 565–574.
[22] S. Andrieux, T.N. Baranger, Three-dimensional recovery of stress intensity factors and energy release rates from surface full-field displacements, Int. J. Solids Struct. 50 (10) (2013) 1523–1537.
[23] T. Baranger, S. Andrieux, R. Rischette, Combined energy method and regularisation to solve the Cauchy problem for the heat equation, Inverse Probl. Sci. Eng. 22 (1) (2014) 199–212.
[24] S. Andrieux, T.N. Baranger, Energy methods for Cauchy problems of evolutions equations, J. Phys. Conf. Ser. 135 (2008) 012007.
[25] R. Rischette, T.N. Baranger, N. Debit, Numerical analysis of an energy-like minimisation method to solve a parabolic Cauchy problem with noisy data, J. Comput. Appl. Math. 271 (2014) 206–222.
[26] J. Hadamard, Lectures on Cauchy's Problem in Linear Partial Differential Equation, Dover, New York, 1953.
[27] B. Belgacem, Why is the Cauchy problem severely ill posed?, Inverse Probl. 23 (2) (2007) 823–836.
[28] S. Andrieux, T.N. Baranger, Solving Cauchy problems for nonlinear hyperelasticity, in: K. Alain, D. Eduardo A. (Eds.), 7th International Conference on Inverse Problems in Engineering, University of Central Florida in Orlando, 26 April 2011, CENTECORP Publishing, University of Central Florida, Orlando, FL, USA, 2011, pp. 191–196.
[29] S. Andrieux, T.N. Baranger, Energy error based numerical algorithms for Cauchy problems for nonlinear elliptic or time dependent operators, in: Inverse Problems Symposium, Michigan State University, East Lansing, MI, USA, 2009.
[30] B. Halphen, Q.S. Nguyen, Sur les matériaux standard généralisés, J. Méc. 14 (1975) 39–63.
[31] P. Mialon, Numerical aspects of the analysis and resolution of elastic-plastic equations, Tech. Rep. Série C, 3, 57-89, EDF E&D Bulletin de la Direction des Études et Recherches, 1986.
[32] J. Simo, T. Hughes, Computational Inelasticity, Interdisciplinary Applied Mathematics: Mechanics and Materials, Springer, 1998.

[33] I. Ekeland, R. Temam, Convex Analysis and Variational Problems, Classics in Applied Mathematics, Society for Industrial and Applied Mathematics, 1976 (SIAM, 3600 Market Street, Floor 6, Philadelphia, PA 19104, USA).
[34] K. Hadj Sassi, S. Andrieux, Parameters identification of a nonlinear viscoelastic model via an energy error functional, in: C. Motasoares, J. Martins, H. Rodrigues, J. Ambrósio, C. Pina, C. Motasoares, E. Pereira, J. Folgado (Eds.), IIIrd European Conference on Computational Mechanics, Springer, Netherlands, 2006, p. 476.
[35] D.C. Drucker, A definition of stable inelastic material, J. Appl. Mech. 26 (1959) 101–195.